ELSEVIER

Chemical Engineering Journal 139 (2008) 2–10

Chemical Engineering Journal

www.elsevier.com/locate/cej

Evaluation of the adsorption kinetics and equilibrium for the potential removal of acid dyes using a biosorbent

Mokhtar Arami [a,b,*], Nargess Yousefi Limaee [a], Niyaz Mohammad Mahmoodi [a,1]

[a] *Department of Organic Colorants, Institute for Colorants, Paint & Coatings, Tehran, Iran*
[b] *Textile Engineering Department, Amirkabir University of Technology, Tehran, Iran*

Received 29 April 2007; received in revised form 7 July 2007; accepted 11 July 2007

Abstract

The adsorption of Acid Red 14 (AR14) and Acid Blue 92 (AB92) onto the microporous and mesoporous egg shell membrane (ESM) was investigated in aqueous solution in a batch system with respect to initial dye concentration, pH, contact time, particle size and biosorbent doses at $20 \pm 1\,^{\circ}C$. The surface area, Fourier transform infrared (FTIR) and scanning electron microscopy (SEM) of ESM were obtained. The surface area of ESM was found to be 2.2098 m^2/g. The pseudo-first-order, pseudo-second-order kinetics and the intraparticle diffusion models were used to describe the kinetics data. The rate constants at different pH values (2–12) were evaluated. The experimental data fitted well to the pseudo-second-order kinetics model at pH values of 2–8 and pseudo-first-order kinetics model at pH values of 10 and 12 for both dyes. Equilibrium isotherms were analyzed by Langmuir, Freundlich and Redlich–Peterson adsorption models. Maximum desorption of ≥89.6% was achieved for AR14 and 82.8% for AB92 in aqueous solution at pH 12. The results indicate that ESM could be fruitfully employed as effective biomaterial for the removal of residual color from effluents.

Keywords: Biosorbent; Acid dye; ESM; Isotherms; Kinetics; Dye removal

1. Introduction

The textile dyeing industry consumes large quantities of water at its different steps of dyeing, finishing, etc. processes. Due to the large volume of water consumption, the production of huge volume of wastewaters is inevitable. Generally, the wastewater from printing and dyeing units in a textile plant is rich in color, containing residue of dyes and chemicals. Due to more and more increasingly stringent restrictions on the hazardous organic content of industrial effluents, it is necessary to eliminate organic pollutants by proper treatment methods before being released it into the water courses [1–3]. Various techniques, such as adsorption [4,5], nanophotocatalysis [6–13], electrochemical [14], membrane processes [15], etc. have been used for the removal of organics as well as inorganics from wastewaters. The non-degradable nature of dyes and their stability toward light and oxidizing agents complicate the selection of a suitable method for their removal. In comparison to the removal methods of colors, it has been well established that adsorption is the most convenient and effective technique to remove color from wastewater [16]. Adsorption is considered to be relatively superior to other techniques because of its low cost, simplicity of design, high efficiency, availability and ability to separate wide range of chemical compounds [17,18].

It is considered that one of the major challenges faced with adsorption by activated carbon is its cost effectiveness. So, the research of the recent years mainly focused on utilizing natural materials as alternatives to activated carbon [19–21]. Several natural adsorbents, such as peat [22], banana peel [23], orange peel [24], rice husk [5], eucalyptus bark [25] and bagasse pith [26] are some of the waste materials which have been tried for this purpose. The acid dyes are one of the most important and widely used dye groups in the textile dyeing industries. However, only a limited number of studies on the removal of AR14 and AB92 dyes have been found in literature [5,27–29]. AR14 and AB92 are water-soluble dyes with high solubility and thus difficult to remove by common chemical treatment methods. Keeping these

* Corresponding author at: Textile Engineering Department, Amirkabir University of Technology, Tehran, Iran. Tel.: +98 21 64542614; fax: +98 21 66400245.
E-mail addresses: mokhtar_arami@yahoo.com (M. Arami), nm_mahmoodi@yahoo.com (N.M. Mahmoodi).
[1] Tel.: +98 21 22956126; fax: +98 21 22947535.

1385-8947/$ – see front matter © 2007 Elsevier B.V. All rights reserved.
doi:10.1016/j.cej.2007.07.060

Nomenclature

AR14	Acid Red 14
AB92	Acid Blue 92
C_e	equilibrium concentration of dye solution
ESM	egg shell membrane
FTIR	Fourier transform infrared
I	intercept
k	equilibrium rate constant of pseudo-second order (g/mmol min)
k_p	intraparticle diffusion rate constant
k_1	equilibrium rate constant of pseudo-first-order kinetics (min^{-1})
K_L	Langmuir constant
K_F	Freundlich constant
K_R and a_R	Redlich–Peterson isotherm constants
$1/n$	adsorption intensity
m_S	optimum amount of ESM (g/L)
pH_0	initial pH
PS	particle size
q_e	amount of dye adsorbed at equilibrium (mmol/g)
q_t	amount of dye adsorbed at time t (mmol/g)
Q_0	maximum adsorption capacity
R^2	goodness of fit criterion
R_L	equilibrium parameter
SEM	scanning electron microscopy
S	agitation speed (rpm)

Greek letter

β	exponent

in mind, it necessitates an attempt to find and provide an easy, feasible and reliable method for their removal, thus utilization of adsorption technique seems to be more fruitful. The focus of this research is to evaluate the adsorption potential of natural biosorbent (ESM) toward the colored compounds. In this respect, acid dyes, Acid Red 14 and Acid Blue 92, was studied as model compounds. ESM is located on the inner surface of the shell, which contains polysaccharides and polypeptides [30]. The effects of particle size and dose of ESM, pH, contact time and initial dye concentration on the adsorption of acid dyes onto ESM were investigated. The Langmuir, Freundlich and Redlich–Peterson isotherms were used to fit the equilibrium data. Pseudo-first-order kinetics, pseudo-second-order kinetics and intraparticle diffusion models were attempted.

2. Experimental

2.1. Chemicals and methods

ESM were supplied by local confectionary. Acid dyes (AR14 and AB92) were provided by Ciba and were used without further purification. The chemical specifications of these dyes are shown in Fig. 1. All other chemicals were of Analar grade and purchased from Merck. The pH measurements were made using

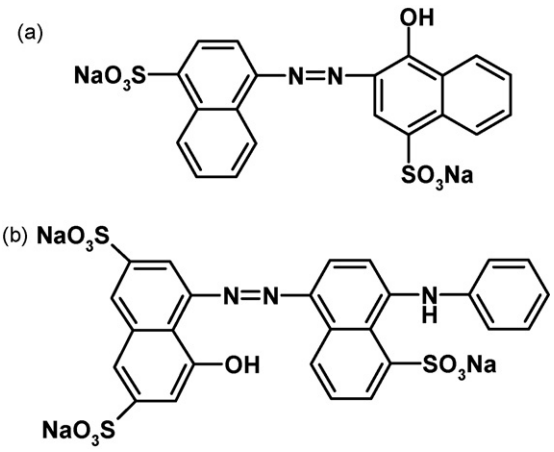

Fig. 1. Chemical structure of (a) Acid Red 14 (C.I. No: 14720, Monoazo, λ_{max} = 517.0) and (b) Acid Blue 92 (C.I. No: 13390, Monoazo, λ_{max} = 595.0).

a pH meter (Hach). UV–vis spectrophotometer CECIL 2021 was employed for absorbance measurements of samples. The maximum wavelength (λ_{max}) used for determination of residual concentration of AR14 and AB92 at pH_0 (initial pH solution) 2 in solution were 517.0 and 595.0 nm, respectively. The dye sample solutions were centrifuged for 20 min in a Hettich EBA20 centrifuge (5000 rpm) prior to adsorption measurements. The FTIR spectrum of ESM was prepared with Perkin-Elmer Spectrophotometer Spectrum One in the range of 450–4000 cm^{-1}.

Scanning electron microscope of untreated ESM and adsorbed ESM with AR14 and AB92 dyes for comparison were obtained using LEO 1455VP scanning microscope. After equilibration, the ESM treated samples were removed from the dye solution, filtered and dried for the SEM analysis. The surface area of ESM was obtained by using the Brunauer, Emmett and Teller (BET) method with Gemini 2375 micrometrics instrument. The surface area of ESM was found to be 2.2098 m^2/g.

2.2. Sample preparation

For the preparation of the ESM, a 25% aqueous acetic acid solution was first used to dissolve the egg shell. The membrane was then taken out of the beaker and cleaned with fresh distilled water twice and dried. The dried membrane was ground and sieved to the required particle size of <0.125 mm.

The adsorption measurements were conducted by mixing various amounts of ESM (0.015–1.2 g) for AR14 and AB92 in jars containing 250 mL of a dye solution (AR14: 0.199 mmol/L, AB92: 0.144 mmol/L) at various pH_0 (2–12). The pH of the solution was adjusted by adding a small amount of HCl or NaOH (1 M). Dye solutions were prepared using distilled water to prevent and minimize possible interferences. Although in actual cases, the dye wastewater will has a different ionic strength and organics present.

Adsorption experiments were carried out at various concentrations of dye solutions using optimum amount of ESM (m_S = 0.4 g/L) at pH_0 2, agitation speed (S) of 200 rpm at 20 ± 1 °C for 2 h to attain the equilibrium conditions. The absorbance of all samples were monitored and determined at

certain time intervals (5, 10, 15, 20, 25, 30, 45, 60 and 120 min) during the adsorption process. The equilibrium was established after 60 min. At the end of the adsorption experiments, the samples were centrifuged and the dye concentration was determined. The results were verified with the Langmuir, Freundlich and Redlich–Peterson adsorption isotherms.

2.3. Desorption studies

The biosorbent that was used for the adsorption of dye solution was separated from solution by filtration and then were dried. It was agitated with 250 mL of distilled water at different pH_0 values (2–12) and agitation speed of 200 rpm for the predetermined equilibrium time of adsorption process.

3. Results and discussion

3.1. Surface characteristics

In order to investigate the surface characteristics of ESM, Fourier transform infrared (FTIR, Perkin-Elmer Spectrophotometer Spectrum One) in the range 450–4000 cm^{-1} was studied (Fig. 2). The FTIR spectrum of ESM shows that the peak positions are at 3411.57, 1648.73, 1528.48, 1308.03 and 1168.70 cm^{-1}. The bands at 3411.57 are due to O–H and N–H stretching. While the bands at 1648.73 and 1528.48 reflect the carbonyl group stretching (amide) and N–H bending, respectively. Bands at 1308.03 and 1168.70 correspond to C–H bending and C–O stretching, respectively [31,32].

3.2. Effect of adsorbent dosage

The effect of ESM doses on the amount of dye adsorbed was investigated by contacting 250 mL of dye solution with initial dye concentration of 0.199 mmol/L of AR14 and 0.144 mmol/L of AB92 using jar test at room temperature (20 ± 1 °C) for 120 min at a constant stirring speed of 200 rpm. Different amounts of ESM (0.06–0.4 g/L) for AR14 and AB92 were applied. After equilibrium, the samples were centrifuged and the concentration in the supernatant dye solution was analyzed. The plot of dye removal (%) versus adsorbent dosage (g/L) is shown in Fig. 3.

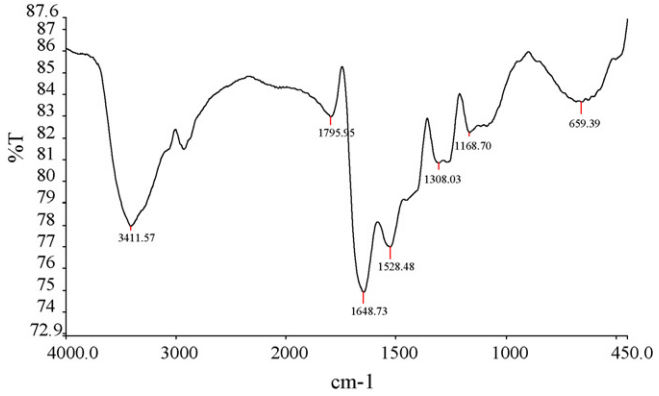

Fig. 2. Fourier transform infrared (FTIR) spectrum of ESM.

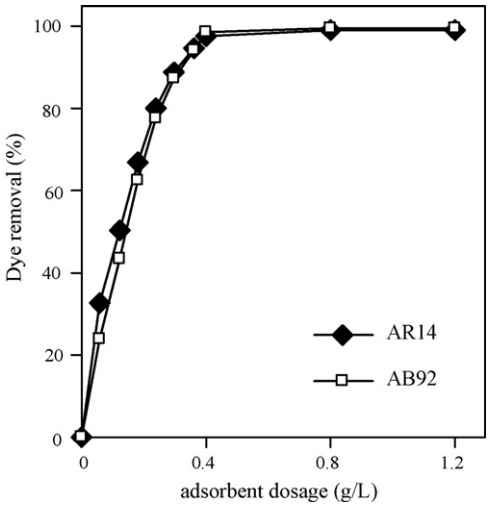

Fig. 3. Effect of adsorbent dosage on the adsorption of dyes on ESM. *Conditions*: pH_0 2, *T* 20 ± 1 °C, *S* 200 rpm, dye concentration (AR14: 0.199 mmol/L, AB92: 0.144 mmol/L) and particle size = <0.125 mm.

3.3. Effect of contact time

The adsorption efficiency of ESM towards AR14 and AB92 were evaluated by determining the percentage decrease of the absorbance at 517.0 and 595 nm, respectively. The influence of varying the initial dye concentration was assessed (Figs. 4 and 5).

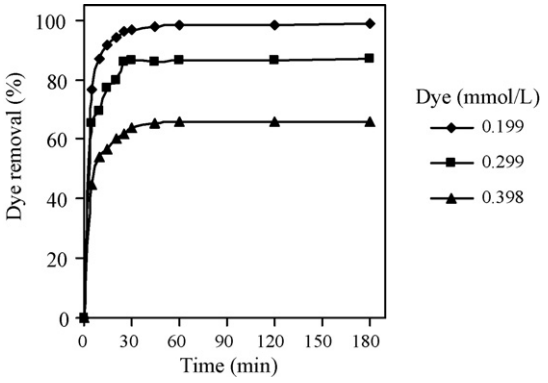

Fig. 4. The effect of contact time and initial dye concentration on AR14 removal by ESM. *Conditions*: pH_0 2, *T* 20 ± 1 °C, *S* 200 rpm, m_s = 0.4 g/L and particle size = <0.125 mm.

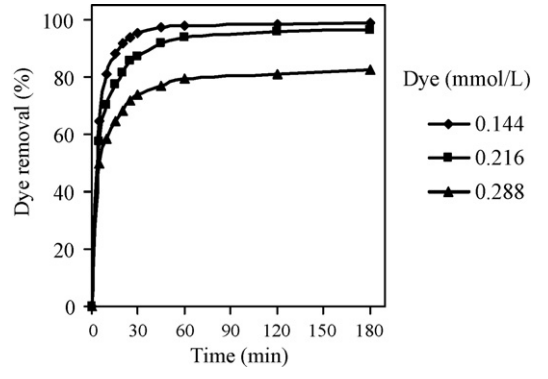

Fig. 5. The effect of contact time and initial dye concentration on AB92 removal by ESM. *Conditions*: pH_0 2, *T* 20 ± 1 °C, *S* 200 rpm, m_s = 0.4 g/L and particle size = <0.125 mm.

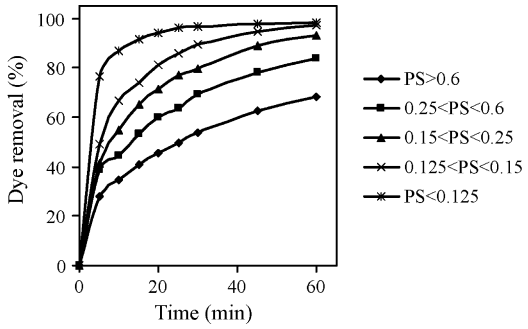

Fig. 6. The effect of adsorbent particle size on the adsorption of AR14 on ESM. *Conditions*: pH_0 2, *T* 20 ± 1 °C, *S* 200 rpm, m_s = 0.4 g/L.

It can be concluded that the percentage of dye adsorption is decreased by increasing the initial dye concentration.

3.4. Effect of particle size

The adsorption of both dyes at different particle sizes, PS < 0.125, 0.125–0.15, 0.15–0.25, 0.25–0.6 and PS > 0.6 was studied. The results are shown in Figs. 6 and 7. It is seen that with decreased particle size, the adsorption increases to some extent. Due to sufficient adsorption capacity, all further studies were carried out using PS < 0.125.

3.5. Effect of pH

The results of blank dye solution studies indicated that, change of the initial pH (pH_0) of dye solution has negligible effect on the λ_{max} of AR14 and AB92 dyes (pH_0 2–12) and during the experiments the pH of dye solutions was not changed significantly. This observation proved that, at this range of pH, there is not occurred any chemical structural change of dye molecules. Based on this observation and assuming negligible dissociation of adsorbent, the pH of all dye solutions were reported as initial pH and pH control during all experiments was ignored. The maximum absorbance wavelength (λ_{max} (nm)) of AR14 and AB92 at different pH_0 values are shown in Table 1.

The effect of initial pH on the adsorption of AR14 and AB92 onto ESM is shown in Fig. 8. The adsorption capacity increases when the pH is decreased. Maximum adsorption of acid dyes

Table 1
The effect of initial pH of dye solutions on the maximum absorbance wavelength (λ_{max} (nm)) of AR14 and AB92

pH	λ_{max} (nm)	
	AR14	AB92
2	517.0	595.0
4	516.5	578.0
6	516.5	575.5
8	513.0	575.0
10	507.0	573.0
12	510.0	574.0

occurs at acidic pH (pH_0 2). ESM is comprised of various functional groups, such as amine, hydroxyl and carbonyl groups which are affected by the pH of solutions. In other words, the predominant charges on the ESM are positive and because of having SO_3^- group in the structure of dyes, it seems the dominant mechanism of the adsorption is electrostatic attraction. Therefore, at various pH values, the electrostatic attraction as well as the ionic property and structure of dye molecules and ESM could play very important roles in dye adsorption on ESM. At pH_0 2, a considerable high electrostatic attraction exists between the positively charged surface of the adsorbent, due to the ionization of functional groups of adsorbent and negatively charged anionic dye molecules. As the pH of the system increases, the number of negatively charged sites are increased. A negatively charged site on the adsorbent does not favor the adsorption of anionic dyes due to the electrostatic repulsion [4,33]. Also, lower adsorption of AR14 and AB92 dyes at alkaline pH is due to the presence of excess OH^- ions destabilizing anionic dyes and competing with the dye anions for the adsorption sites. Thus, the effective pH_0 was 2 and it was used in further studies. Similar results of pH effect were also reported for the adsorption of acid yellow 36 and Congo red onto agricultural wastes [33].

3.6. Adsorption kinetics

Several models can be used to express the mechanism of solute sorption onto a sorbent. In order to design a fast and effective model, investigations were made on adsorption rate. For the examination of the controlling mechanisms of adsorption

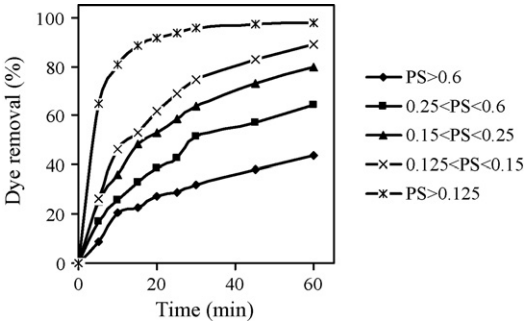

Fig. 7. The effect of adsorbent particle size on the adsorption of AB92 on ESM. *Conditions*: pH_0 2, *T* 20 ± 1 °C, *S* 200 rpm, m_s = 0.4 g/L.

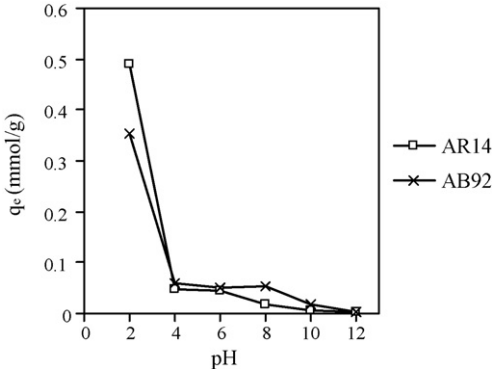

Fig. 8. Effect of pH for the adsorption of AR14 and AB92 on ESM. *Conditions*: *T* 20 ± 1 °C, *S* 200 rpm, particle size = <0.125 mm and equilibrium time = 120 min.

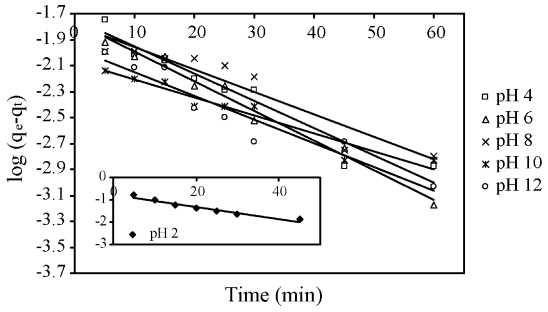

Fig. 9. Pseudo-first-order sorption kinetics of AR14 onto ESM. *Conditions*: T 20 ± 1 °C, S 200 rpm, particle size = <0.125 mm and m_s = 0.4 g/L.

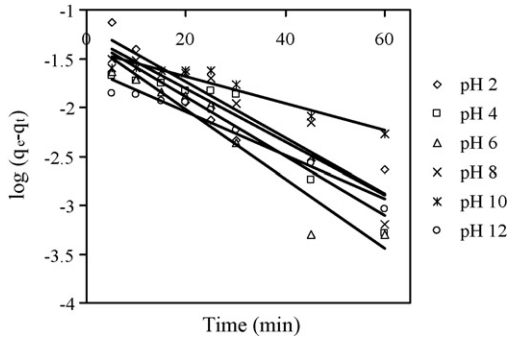

Fig. 10. Pseudo-first-order sorption kinetics of AB92 onto ESM. *Conditions*: T 20 ± 1 °C, S 200 rpm, particle size = <0.125 mm and m_s = 0.4 g/L.

process, such as chemical reaction, diffusion control and mass transfer, several kinetics models are used to test the experimental data [34,35].

3.6.1. 3.6.1.Pseudo-first-order equation

Pseudo-first-order equation is generally represented as follows [36,37]:

$$\frac{dq_t}{dt} = k_1(q_e - q_t) \tag{1}$$

where q_e is the amount of dye adsorbed at equilibrium (mmol/g), q_t the amount of dye adsorbed at time t (mmol/g) and k_1 is the equilibrium rate constant of pseudo-first-order kinetics (1/min). After integration by applying conditions, $q_t = 0$ at $t = 0$ and $q_t = q_t$ at $t = t$, then Eq. (1) becomes

$$\log(q_e - q_t) = \log(q_e) - \frac{k_1}{2.303}t \tag{2}$$

The straight-line plots of $\log(q_e - q_t)$ versus t (Figs. 9 and 10) for the adsorption of AR14 and AB92 onto ESM at different pHs (2–12) have also been tested to obtain the rate parameters. The k_1, q_e and correlation coefficients under different pH values were calculated from these plots and are given in Table 2.

3.6.2. Pseudo-second-order equation

Data were applied to the Ho and MaKay's pseudo-second-order chemisorption kinetic rate equation which is expressed as [36,38]:

$$\frac{dq_t}{dt} = k(q_e - q_t) \tag{3}$$

where q_e is amount of dye adsorbed at equilibrium (mmol/g) and k is the equilibrium rate constant of pseudo-second order (g/mmol min). On integrating the Eq. (3),

$$\frac{t}{q_t} = \frac{1}{kq_e^2} + \frac{1}{q_e}t \tag{4}$$

To understand the applicability of the model, a linear plots of t/q_t versus t under different pH_0 values (2–12) for the adsorption of AR14 and AB92 onto ESM are shown in Figs. 11 and 12. The k, q_e and correlation coefficients were calculated from these plots and are given in Table 2. From Table 2, adsorption kinetics of dyes was studied and the rates of sorption were found to conform to pseudo-second-order kinetics with good correlation for the pH values of 2–8. These obedience from pseudo-second-order kinetics, might be attributed to the activity of H^+ together with dye ions at acidic-neutral pHs. For the pHs 10 and 12,

Table 2
Kinetics constants for pseudo-first- and pseudo-second-order models

Dye	Pseudo-first order			Pseudo-second order			Intraparticle diffusion model		
	k_1 (1/min)	q_e (mmol/g)	R^2	k (g/mmol min)	q_e (mmol/g)	R^2	k_p	I	R^2
AR14									
pH = 2	0.0626	0.1768	0.9545	0.7822	0.49928	**0.9998**	0.0442	0.2383	0.9095
pH = 4	0.0481	0.0179	0.9335	5.9891	0.05409	**0.9991**	0.002	0.0372	0.9471
pH = 6	0.0525	0.01703	0.9791	6.495	0.04774	**0.9982**	0.0022	0.0301	0.9391
pH = 8	0.0398	0.01644	0.8914	4.1617	0.02714	**0.9672**	0.0021	0.0081	0.9292
pH = 10	0.0320	0.0085	**0.9277**	0.0605	−0.04258	0.0313	0.0017	0.0016	0.9023
pH = 12	0.0424	0.0108	**0.9135**	0.7694	0.02237	0.5598	0.0011	0.0022	0.9422
AB92									
pH = 2	0.0624	0.0537	0.8633	2.3235	0.36415	**0.9999**	0.024	0.2376	0.9375
pH = 4	0.06955	0.0508	0.8896	2.098	0.06494	**0.9747**	0.0025	0.0333	0.9657
pH = 6	0.08153	0.04798	0.9188	2.1677	0.05812	**0.9903**	0.0047	0.0179	0.9817
pH = 8	0.06564	0.06803	0.8761	0.9494	0.06545	**0.9531**	0.0044	0.0127	0.9375
pH = 10	0.03132	0.03828	**0.9013**	0.7196	−0.0139	0.2577	0.0005	0.0004	0.8605
pH = 12	0.05113	0.02522	**0.9484**	0.0406	−0.0738	0.1088	0.0016	−0.0027	0.9236

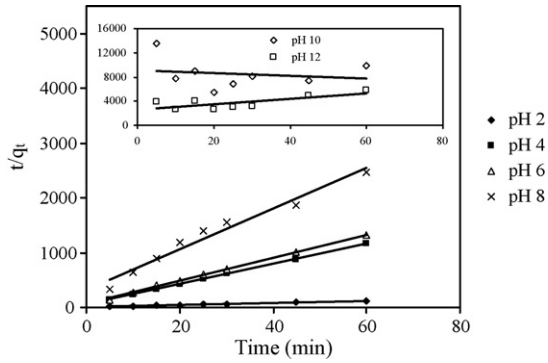

Fig. 11. Pseudo-second-order sorption kinetics of AR14 onto ESM. *Conditions*: T 20 ± 1 °C, S 200 rpm, particle size = <0.125 mm and m_s = 0.4 g/L.

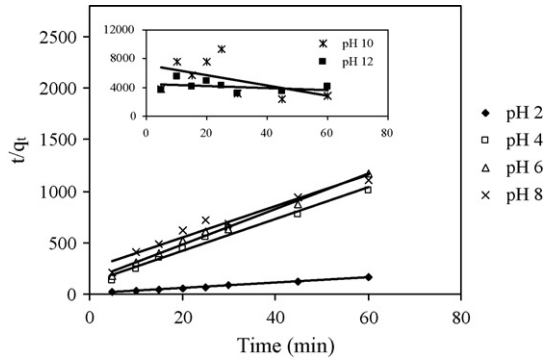

Fig. 12. Pseudo-second-order sorption kinetics of AB92 onto ESM. *Conditions*: T 20 ± 1 °C, S 200 rpm, particle size = <0.125 mm and m_s = 0.4 g/L.

the rate of sorption follows the pseudo-first-order kinetics with good correlation. It seems that at high pH values OH^- ion is a dominant adsorbed species.

3.6.3. The intraparticle diffusion model

The possibility of intraparticle diffusion resistance affecting adsorption was explored by using the intraparticle diffusion model as

$$q_t = k_p t^{1/2} + I \tag{5}$$

where k_p is the intraparticle diffusion rate constant. In Figs. 13 and 14, a plot of mass of AR14 and AB92 adsorbed

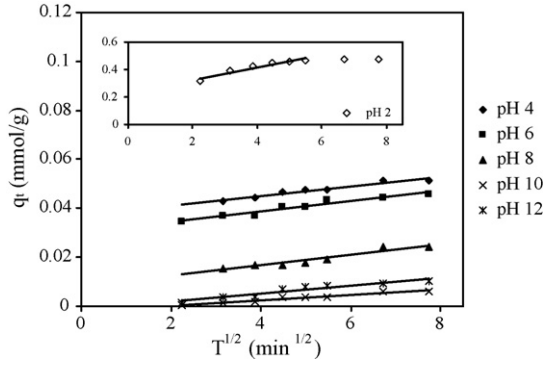

Fig. 13. Intraparticle diffusion plots for the removal of AR14 by ESM. *Conditions*: T 20 ± 1 °C, S 200 rpm, particle size = <0.125 mm and m_s = 0.4 g/L.

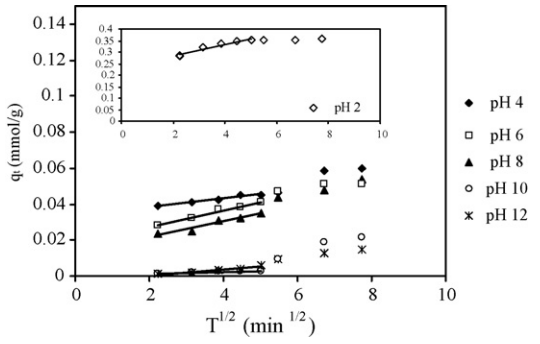

Fig. 14. Intraparticle diffusion plots for the removal of AB92 by ESM. *Conditions*: T 20 ± 1 °C, S 200 rpm, particle size = <0.125 mm and m_s = 0.4 g/L.

per unit mass of adsorbent, q_t versus $t^{1/2}$ is presented for pH_0 values of 2–12. Values of I (Table 2) give an idea about the thickness of the boundary layer, i.e., the larger intercept the greater is the boundary layer effect. According to this model, the plot of uptake, should be linear if intraparticle diffusion is involved in the adsorption process and if these lines pass through the origin then intraparticle diffusion is the rate controlling step [21,39–41]. When the plots do not pass through the origin, this is indicative of some degree of boundary layer control and this further shows that the intraparticle diffusion is not the only rate-limiting step, but also other kinetic models may control the rate of adsorption, all of which may be operating simultaneously. The slope of linear portion from Figs. 13 and 14 can be used to derive values for the rate parameter, k_p, for the intraparticle diffusion, given in Table 2. The correlation coefficients for intraparticle diffusion model are between 0.8605 and 0.9817.

3.7. Adsorption isotherms

To optimize the design of an adsorption system for the adsorption of adsorbates, it is important to establish the most appropriate correlation for the equilibrium curves. Various isotherm equations like those of Langmuir, Freundlich and Redlich–Peterson adsorption isotherms were tested in this work. In the Langmuir theory, the basic assumption is that the sorption takes place at specific homogeneous sites within the adsorbent. This equation can be written as follows [42–47]:

$$q_e = \frac{Q_0 K_L C_e}{1 + K_L C_e} \tag{6}$$

where q_e is the amount of dye adsorbed on ESM at equilibrium, C_e the equilibrium concentration of dye solution, K_L the equilibrium constant and Q_0 is the maximum adsorption capacity.

The linear form of Langmuir equation is:

$$\frac{C_e}{q_e} = \frac{1}{K_L Q_0} + \frac{C_e}{Q_0} \tag{7}$$

the essential characteristic of the Langmuir isotherm can be expressed by the dimensionless constant called equilibrium parameter, R_L, defined by

$$R_L = \frac{1}{1 + K_L C_0} \tag{8}$$

Table 3
Linearized isotherm coefficients for dyes

Langmuir constants				
Dye	Q_0	K_L	R_L	R^2
AR14	1.023	56.497	0.082	0.826
AB92	0.545	244.738	0.028	0.903

Freundlich constants			
Dye	K_F	$1/n$	R^2
AR14	1.797	0.303	0.900
AB92	0.789	0.156	0.991

Redlich–Peterson constants				
Dye	K_R	a_R	β	R^2
AR14	293714.7	349186.2	0.897703	**0.992**
AB92	758653.5	481025.2	0.633962	**0.998**

where K_L is the Langmuir constant and C_0 is the initial dye concentration (mmol/L), R_L values indicate the type of isotherm to be irreversible ($R_L = 0$), favorable ($0 < R_L < 1$), linear ($R_L = 1$) or unfavorable ($R_L > 1$) [24,48]. The R_L values for the adsorption of AR14 and AB92 on ESM have been shown in Table 3.

The Freundlich isotherm is derived by assuming a heterogeneous surface with a non-uniform distribution of heat of adsorption over the surface. Freundlich isotherm can be expressed by [45–47,49]:

$$q_e = K_F C_e^{1/n} \tag{9}$$

where K_F is adsorption capacity at unit concentration and $1/n$ is adsorption intensity. $1/n$ values indicate the type of isotherm to be irreversible ($1/n = 0$), favorable ($0 < 1/n < 1$), unfavorable ($1/n > 1$) [45]. Eq. (4) can be rearranged to a linear form:

$$\log q_e = \log K_F + \left(\frac{1}{n}\right) \log C_e \tag{10}$$

The $1/n$ values for the Freundlich adsorption isotherm have been shown in Table 3.

The Redlich–Peterson isotherm model combines elements from both the Langmuir and Freundlich equations, and the mechanism of adsorption is a hybrid one and does not follow ideal monolayer adsorption. The Redlich–Peterson equation is widely used as a compromise between Langmuir and Freundlich systems. It is expressed as [21,49–53]:

$$q_e = \frac{K_R C_e}{1 + a_R C_e^{\beta}} \tag{11}$$

K_R and a_R are the Redlich–Peterson isotherm constants and β is the exponent, which lies between 0 and 1.

The Redlich–Peterson isotherm incorporates three parameters and can be applied either in homogeneous or heterogeneous systems. Eq. (11) can be converted to

$$\ln\left(K_R \frac{C_e}{q_e} - 1\right) = \ln a_R + \beta \ln C_e \tag{12}$$

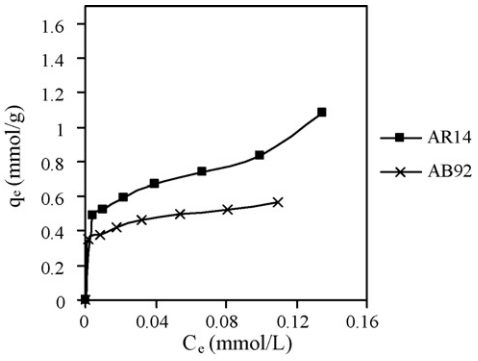

Fig. 15. Adsorption isotherms of dyes using ESM. *Conditions*: pH_0 2, T 20 ± 1 °C, S 200 rpm, particle size = <0.125 mm and equilibrium time = 60 min.

A minimization procedure has been adopted to solve Eq. (12) by maximizing the correlation coefficient between the predicted values of q_e from Eq. (12) and the experimental data using the solver add-in function of the MS excel.

Fig. 15 shows the adsorption isotherms of dyes (q_e versus C_e) using ESM. The values of R^2 (goodness of fit criterion) computed by linear regression for the all investigated types of isotherms are presented in Table 3. The data of Table 3 indicate that the Redlich–Peterson isotherm is most appropriate for adsorption of AR14 and AB92 on ESM.

3.8. Desorption studies

Desorption studies help to elucidate the mechanism and recovery of the adsorbate and adsorbent. As the pH of desorbing solution was increased, the percent desorption increased from 1% at pH_0 2 to ≥89.6% at pH_0 12 for AR14 and from 1.6% at pH_0 2 to 82.8% at pH_0 12 for AB92 (Fig. 16).

As the pH of the system increases, the number of negatively charged sites increased. A negatively charged site on the adsorbent favors the desorption of dye anions due to the electrostatic repulsion [33,54]. At pH_0 12, a significantly high electrostatic repulsion exists between the negatively charged surface of the adsorbent and anionic dye.

3.9. SEM analysis

Scanning electron microscopy (SEM) has been a primary tool for characterizing the surface morphology and fundamental

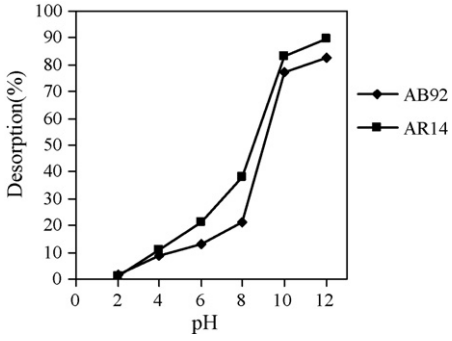

Fig. 16. Effect of pH on desorption of AR14 and AB92 on ESM. *Conditions*: T 20 ± 1 °C, S 200 rpm.

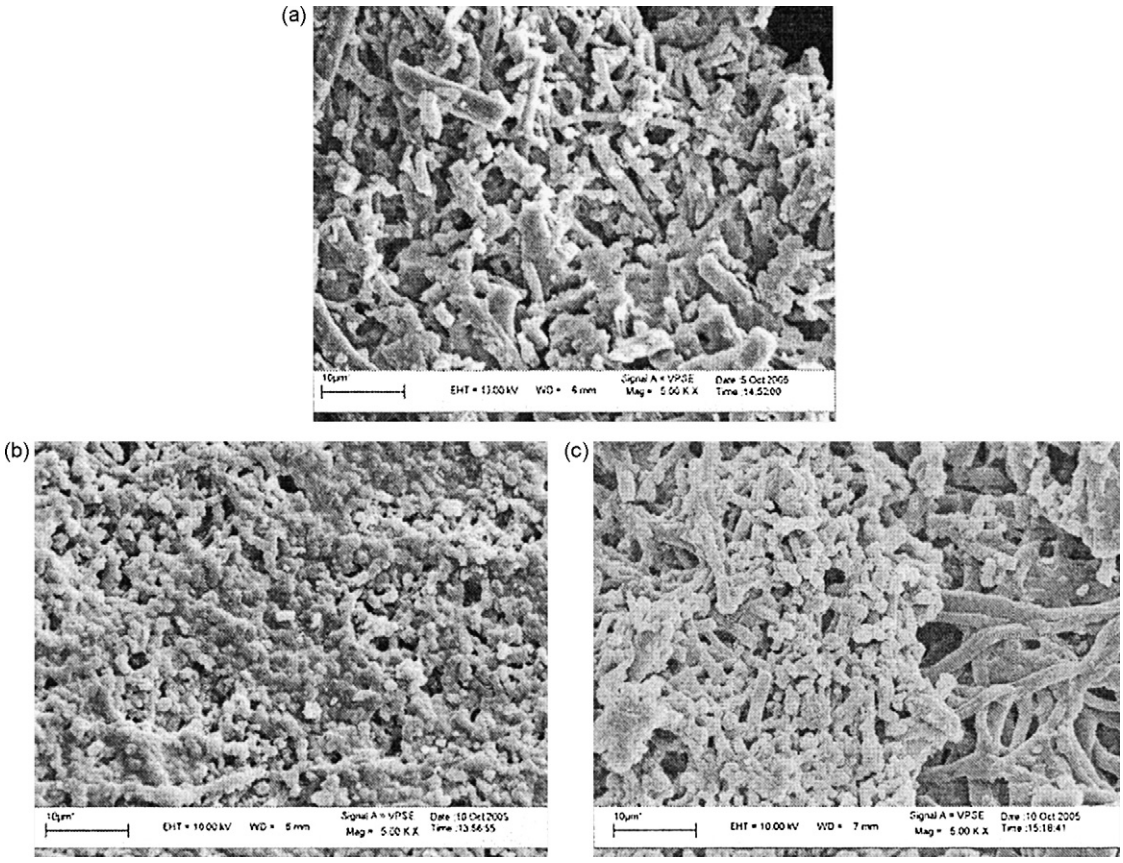

Fig. 17. SEM images for ESM: (a) original ESM; (b) after 60 min adsorption process (AR14) and (c) after 60 min adsorption process (AB92). *Conditions*: 0.4 g/L of ESM for AR 14 and AB 92, (AR14: 0.199 mmol/L, AB92: 0.144 mmol/L), equilibrium time = 60 min, *S* 200 rpm, *T* 20 ± 1 °C, and particle size = <0.125 mm.

physical properties of the adsorbent surface. It is useful for determining the particle shape, porosity and appropriate size distribution of the adsorbent. Scanning electron micrographs of raw ESM and adsorbed ESM with AR14 and AB92 are shown in Fig. 17. From Fig. 17, it is clear that, ESM has considerable numbers of pores where, there is a good possibility for dyes to be trapped and adsorbed into these pores. The SEM pictures of ESM samples show very distinguished dark spots which can be taken as a sign for effective adsorption of dye molecules in the cavities and pores of this adsorbent.

4. Conclusion

Equilibrium and kinetic studies were done for the adsorption of Acid Red 14 (AR14) and Acid Blue 92 (AB92) from aqueous solutions onto ESM. Results of adsorption showed that ESM, can be effectively used as a biosorbent for the removal of model anionic dyes. This biosorbent exhibited high sorption capacities toward AR14 and AB92. The kinetics studies of dyes on ESM were performed based on pseudo-first order, pseudo-second order and intraparticle diffusion rate mechanism. The data indicate that the adsorption kinetics of dyes on ESM followed the pseudo-second-order rate expression at the pH values of 2–8 and obeyed the pseudo-first-order rate expression at the pH values of 10 and 12. The equilibrium data have been analyzed using Langmuir, Freundlich and Redlich–Peterson isotherms and the characteristic parameters for each isotherm have been determined. The results showed that the experimental data were correlated reasonably well by the Redlich–Peterson adsorption isotherm. Desorption studies were conducted and the results showed that at alkaline pH values high electrostatic repulsion existed between the negatively charged surface of the adsorbent and anionic dye.

References

[1] S. Chakraborty, S. De, J.K. Basu, S. DasGupta, Treatment of a textile effluent: application of a combination method involving adsorption and nanofiltration, Desalination 174 (2005) 73–85.
[2] G. Crini, Non-conventional low-cost adsorbents for dye removal: a review, Bioresour. Technol. 97 (2006) 1061–1085.
[3] R. Sanghi, B. Bhattacharya, Review on decolorisation of aqueous dye solutions by low cost adsorbents, Color. Technol. 118 (2002) 256–269.
[4] M. Arami, N.Y. Limaee, N.M. Mahmoodi, N.S. Tabrizi, Removal of dyes from colored textile wastewater by orange peel adsorbent: equilibrium and kinetics studies, J. Colloid Interface Sci. 288 (2005) 371–376.
[5] M. Arami, N.Y. Limaee, N.M. Mahmoodi, N.S. Tabrizi, Equilibrium and kinetics studies for the adsorption of direct and acid dyes from aqueous solution by soy meal hull, J. Hazard. Mater. B 135 (1–3) (2006) 171–179.
[6] N.M. Mahmoodi, M. Arami, N.Y. Limaee, K. Gharanjig, F.D. Ardejani, Decolorization and mineralization of textile dyes at solution bulk by heterogeneous nanophotocatalysis using immobilized nanoparticles of titanium dioxide, Colloids Surf. A Physicochem. Eng. Aspects 290 (2006) 125–131.
[7] N.M. Mahmoodi, M. Arami, N.Y. Limaee, N.S. Tabrizi, Decolorization and aromatic ring degradation kinetics of Direct Red 80 by UV oxidation in the presence of hydrogen peroxide utilizing TiO_2 as a photocatalyst, Chem. Eng. J. 112 (1–3) (2005) 191–196.

[8] N.M. Mahmoodi, M. Arami, N.Y. Limaee, Photocatalytic degradation of triazinic ring-containing azo dye (Reactive Red 198) by using immobilized TiO_2 photoreactor: bench scale study, J. Hazard. Mater. B 133 (1–3) (2006) 113–118.
[9] N.M. Mahmoodi, M. Arami, N.Y. Limaee, N.S. Tabrizi, Kinetics of heterogeneous photocatalytic degradation of reactive dyes in an immobilized TiO_2 photocatalytic reactor, J. Colloid Interface Sci. 295 (1) (2006) 159–164.
[10] N.M. Mahmoodi, M. Arami, Bulk phase degradation of Acid Red 14 by nanophotocatalysis using immobilized titanium (IV) oxide nanoparticles, J. Photochem. Photobiol. A Chem. 182 (2006) 60–66.
[11] N.M. Mahmoodi, M. Arami, N.Y. Limaee, K. Gharanjig, F. Nourmohammadian, Nanophotocatalysis using immobilized titanium dioxide nanoparticle. Degradation and mineralization of water containing organic pollutant: case study of Butachlor, Mater. Res. Bull. 42 (2007) 797–806.
[12] N.M. Mahmoodi, N.Y. Limaee, M. Arami, S. Borhany, M. Mohammad-Taheri, Nanophotocatalysis using nanoparticles of titania. Mineralization and finite element modelling of Solophenyl dye decolorization, J. Photochem. Photobiol. A Chem. 189 (2007) 1–6.
[13] N.M. Mahmoodi, M. Arami, N.Y. Limaee, K. Gharanjig, Photocatalytic degradation of agricultural *N*-heterocyclic organic pollutants using immobilized nanoparticles of titania, J. Hazard. Mater. 145 (2007) 65–71.
[14] A. Fernandes, A. Morao, M. Magrinho, A. Lopes, I. Goncalves, Electrochemical degradation of C.I. Acid Orange 7, Dyes Pigments 61 (2004) 287–296.
[15] A. Akbari, J.C. Remigy, P. Aptel, Treatment of textile dye effluents using a polyamide-based nanofiltration membrane, Chem. Eng. Process. 41 (2002) 601–609.
[16] K. Ravikumar, S. Krishnan, S. Ramalingam, K. Balu, Optimization of process variables by the application of response surface methodology for dye removal using a novel adsorbent, Dyes Pigments 72 (1) (2007) 66–74.
[17] N. Kannan, M.M. Sundaram, Kinetics and mechanism of removal of methylene blue by adsorption on various carbons-a comparative study, Dyes Pigments 51 (2001) 25–40.
[18] V. Meshko, L. Markovska, M. Mincheva, A.E. Rodrigues, Adsorption of basic dyes on granular activated carbon and natural zeolite, Water Res. 35 (2001) 3357–3366.
[19] G. Annadurai, R.S. Juang, D.J. Lee, Factorial design analysis for adsorption of dye on activated carbon beads incorporated with calcium alginate, Adv. Environ. Res. 6 (2002) 191–198.
[20] M.S. EL-Geundi, Adsorbents for industrial pollution control, Adsorpt. Sci. Technol. 15 (1997) 777–787.
[21] I.D. Mall, V.C. Srivastava, N.K. Agarwal, I.M. Mishra, Removal of congo red from aqueous solution by bagasse fly ash and activated carbon: kinetic study and equilibrium isotherm analyses, Chemosphere 61 (2005) 492–501.
[22] Y.S. Ho, G. McKay, Sorption of dye from aqueous solution by peat, Chem. Eng. J. 70 (2) (1998) 115–124.
[23] G. Annadurai, R.S. Juang, D.J. Lee, Use of cellulose-based wastes for adsorption of dyes from aqueous solutions, J. Hazard. Mater. B 92 (2002) 263–274.
[24] R. Sivaraj, C. Namasivayam, K. Kadirvelu, Orange peel as an adsorbent in the removal of acid violet 17 (acid dye) from aqueous solutions, Waste Manage. 21 (2001) 105–110.
[25] L.C. Morais, O.M. Freitas, E.P. Gonc Alves, L.T. Vasconcelos, C.G. Gonzaa Lez Bec, Reactive dyes removal from wastewaters by adsorption on eucalyptus bark: variables that define the process, Water Res. 33 (4) (1999) 979–988.
[26] B. Chen, C.W. Hui, G. McKay, Film-pore diffusion modeling and contact time optimization for the adsorption of dyestuffs on pith, Chem. Eng. J. 84 (2001) 77–94.
[27] N. Hoda, E. Bayram, E. Ayranci, Kinetic and equilibrium studies on the removal of acid dyes from aqueous solutions by adsorption onto activated carbon cloth, J. Hazard. Mater. 137 (1) (2006) 344–351.
[28] M.-S. Kim, J.-M. Lee, B. Hwang, W. Bae, B.-W. Kim, Role of adsorption in the photodegradation of a dye, acid-blue 92, Int. J. Environ. Pollut. 27 (1–3) (2006) 247–258.
[29] J.-C. Park, The removal of organic dye waste using natural clay minerals, J. Korean Chem. Soc. 50 (4) (2006) 321–327.
[30] S.J. Allen, M. McCallen, M.G. Healy, M. Wolki, P. Ulbig, The use of egg shell membrane as an adsorbent for the treatment of coloured waste effluents, in: Proceedings of the second Pacific Basin Conference on Adsorption Science and Technology, 14–18 May, 2000, pp. 46–50.
[31] J. He, W. Ma, J. He, J. Zhao, J.C. Yu, Photooxidation of azo dye in aqueous dispersions of H_2O_2/α-FeOOH, Appl. Catal. B Environ. 39 (2002) 211–220.
[32] D.L. Pavia, G.M. Lampman, G.S. Kaiz, Introduction to Spectroscopy: A Guide for Students of Organic Chemistry, W.B. Saunders Company, 1987.
[33] C. Namasivayam, D. Kavitha, Removal of Congo Red from water by adsorption onto activated carbon prepared from coir pith, an agricultural solid waste, Dyes Pigments 54 (2002) 47–58.
[34] Y.S. Ho, Adsorption of heavy metals from waste streams by peat, Ph.D. Thesis, The University of Birmingham, Birmingham, U.K., 1995.
[35] S. Lagergren, Zur theorie der sogenannten adsorption gelöster stoffe, K. Sven. Vetenskapsakad. Handl. 24 (4) (1898) 1–39.
[36] Y.S. Ho, Sorption studies of acid dye by mixed sorbents, Adsorption 7 (2001) 139–147.
[37] Y.S. Ho, Citation review of Lagergren kinetic rate equation on adsorption reactions, Scientometrics 59 (2004) 171–177.
[38] Y.S. Ho, G. McKay, Pseudo-second order model for sorption processes, Process Biochem. 34 (1999) 451–465.
[39] A. Ozcan, A.S. Ozcan, Adsorption of Acid Red 57 from aqueous solutions onto surfactant-modified sepiolite, J. Hazard. Mater. B 125 (2005) 252–259.
[40] S. Senthilkumaar, P. Kalaamani, K. Porkodi, P.R. Varadarajan, C.V. Subburaam, Adsorption of dissolved reactive red dye from aqueous phase onto activated carbon prepared from agricultural waste, Bioresour. Technol. 97 (14) (2006) 1618–1625.
[41] W.J. Weber, J.C. Morris, Kinetics of adsorption on carbon from solution, J. Sanitary Eng. Div. Am. Soc. Civ. Eng. 89 (SA2) (1963) 31–60.
[42] I. Langmuir, The constitution and fundamental properties of solids and liquids. I. Solids, J. Am. Chem. Soc. 38 (1916) 2221–2295.
[43] I. Langmuir, The constitution and fundamental properties of solids and liquids. II. Liquids, J. Am. Chem. Soc. 39 (1917) 1848–1906.
[44] I. Langmuir, The adsorption of gases on plane surfaces of glass, mica and platinum, J. Am. Chem. Soc. 40 (1918) 1361–1403.
[45] E.R. Alley, Water Quality Control Handbook, McGraw-Hill Education, Europe, London, 2000, pp. 125–141.
[46] L.D. Benefield, J.F. Judkins, B.L. Weand, Process Chemistry for Water and Wastewater Treatment, Prentice Hall, Englewood Cliffs, New Jersey, 1982, pp. 191–210.
[47] F. Woodard, Industrial Waste Treatment Handbook, Butterworth-Heinemann, Boston, 2001, pp. 376–451.
[48] K.R. Hall, L.C. Eagleton, A. Acrivos, T. Vermeulen, Pore and solid diffusion kinetics in fixed-bed adsorption under constant pattern conditions, Ind. Eng. Chem. Fundam. 5 (1966) 212–223.
[49] H.M.F. Freundlich, Uber die adsorption in lasugen, Z. Phys. Chem. (Leipzig) 57A (1906) 385–470.
[50] O. Redlich, D.L. Peterson, A useful adsorption isotherm, J. Phys. Chem. 63 (1959) 1024–1026.
[51] S.J. Allen, G. McKay, J.F. Porter, Adsorption isotherm models for basic dye adsorption by peat in single and binary component systems, J. Colloid Interface Sci. 280 (2004) 322–333.
[52] Y.S. Ho, C.T. Huang, H.W. Huang, Equilibrium sorption isotherm for metal ions on tree fern, Process Biochem. 37 (2002) 1421–1430.
[53] S. Wang, Y. Boyjoo, A. Choueib, Z.H. Zhu, Removal of dyes from aqueous solution using fly ash and red mud, Water Res. 39 (1) (2005) 129–138.
[54] F. Yuzhu, T. Viraraghavan, Removal of Congo Red from an aqueous solution by fungus *Aspergillus niger*, Adv. Environ. Res. 7 (2002) 239–247.